Integrated optics ring-resonator chemical sensor with polymer transduction layer

A. Ksendzov, M.L. Homer and A.M. Manfreda

An integrated optics chemical sensor based on a ring resonator with an ethyl cellulose polymer coating has been demonstrated. The measured sensitivity to isopropanol in air is 50 ppm—the level immediately useful for health-related air quality monitoring. The resonator was fabricated using SiO_2 and Si_xN_y materials. The signal readout is based on tracking the wavelength of a resonance peak. The resonator layout optimisation for sensing applications is discussed.

Introduction: While integrated optics ring and disk resonator-based sensors have been discussed and built [1, 2], no gas sensors with practical applications have been demonstrated to our knowledge. Our ring resonators are intended for use with polymer sensing layers. Arrays of polymers are used to identify chemical compounds in a gaseous environment. The technique is based on correlation of the response of several partially specific sensors (polymer films) to a target chemical [3, 4]. Frequently, polymer films are used as conductometric sensors whereby a thin film of insulating polymer is loaded with a conductive medium (carbon black) [3, 5, 6]. When the target chemical is present, the polymer swells, causing a change in conductivity which is used to quantify the response. However, it is not always possible to effectively load a polymer with conductive particles. Optical readout may circumvent this problem as well as provide improved sensitivity, linearity and stability. Our sensors are based on evanescent wave interaction and respond to a combination of swelling and refractive index change of a polymer layer due to the chemical permeating the polymer. The readout is based on tracking the position of a resonance which is a measure of the effective refractive index in the waveguide.

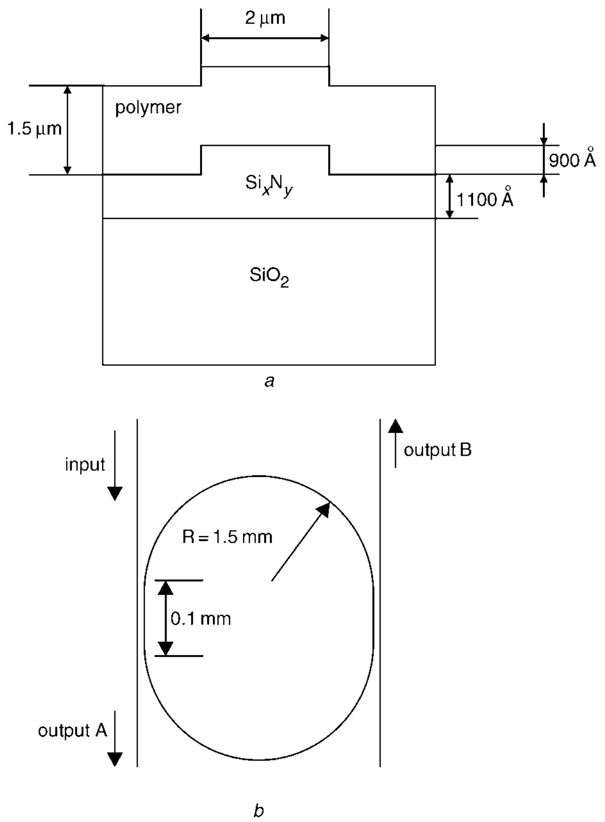

Fig. 1 *Cross-section of waveguide, and schematic diagram of ring resonator*

a Cross-section of waveguide
b Schematic diagram of ring resonator
Waveguide separation between straight section and racetrack structure is 2 μm

Resonator layout and modelling: The waveguide cross-section is shown in Fig. 1*a*. In our device the sensing polymer film also plays the role of the top optical cladding. Refractive indexes of all layers at the operating wavelength of 1570 nm were measured using spectroscopic ellipsometry and are listed in Table 1. The waveguides were designed to ensure significant overlap between the propagating field and the cladding—a confinement factor for the cladding area of 0.35 was calculated. This ensures strong dependence of the effective refractive index of the waveguide n on the refractive index of the top (sensing polymer) cladding N_c—we calculated dn/dN_c of 0.2.

Table 1: Refractive indexes of waveguide layers

Material	SiO_2	Si_xN_y	Ethyl cellulose
Refractive index	1.454 ± 0.004	1.855 ± 0.004	1.451 ± 0.006

The schematic diagram of the ring resonator is shown in Fig. 1*b*. It has a racetrack shape with 1.5 mm bend radius and 0.1 mm straight sections that serve as coupling regions. Based on the waveguide separation in coupling regions of 2 μm, the theoretically predicted power cross-over fraction at 1570 nm wavelength is 0.22. Applying the theoretical treatment of [7] to the measured output spectrum at port A, we computed a cross-over fraction of 0.23 and a loss of 1.5 dB/cm.

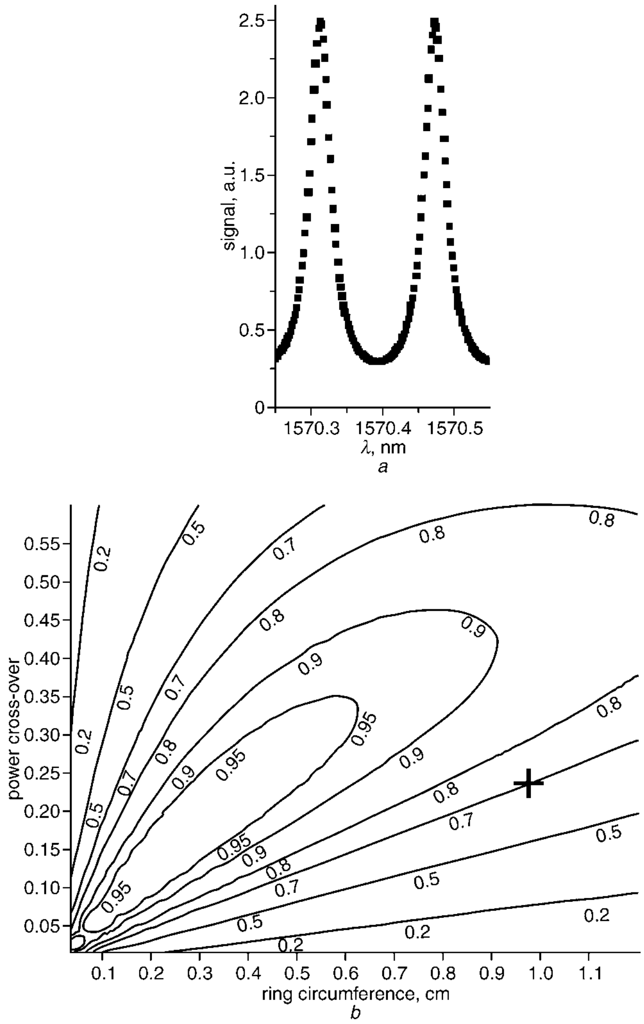

Fig. 2 *Measured output signal of ring-resonator sensor—output B, and steepest slope of resonator output against ring circumference and power cross-over in coupling regions*

a Measured output signal of ring-resonator sensor—output B
b Steepest slope of resonator output against ring circumference and power cross-over in coupling regions
Data scaled to obtain 1 at maximum
+ reported sensor

The design of the race track can be optimised to allow for use of moderately lossy cladding materials in the following fashion. The measured throughput of the resonator (signal out of the port B) is shown in Fig. 2*a*. Since we track the wavelength of a resonance to measure the perturbation, the derivative of the signal against wavelength at the steepest point of this curve must be maximised. In Fig. 2b, we have used the formulae of [7] to plot this quantity for various values of the ring circumference and power cross-over for 1.5 dB/cm optical loss. The results were scaled to obtain 1 at the maximum. The cross corresponds to the reported resonator. Notice that the stated optimisation condition leads to rather relaxed constraints—about one third of the shown design space falls within 80% of the best case.

Fabrication: The ring resonator was fabricated on an Si substrate. First, the lower cladding of 7 μm thermal oxide was grown. Then 0.11 μm of Si_xN_y was grown by plasma enhanced chemical vapour deposition (PECVD) and annealed in N_2 atmosphere at 1100°C followed by the growth of 0.09 μm of PECVD Si_xN_y. The ring was then patterned in photoresist using conventional contact lithography and the pattern was transferred into the top layer of Si_xN_y using commercial buffered oxide etchant (BOE). Owing to high hydrogen content of the PECVD Si_xN_y it is readily patterned in BOE, while the etch rate of the annealed layer is negligible. This layer was then annealed to drive off hydrogen—a step necessary to reduce optical losses. A solution of ethyl cellulose (48% ethoxy content) in 1,3-dioxolane was spread over the resonator using a conventional photoresist spinner. The sensor was then placed on a hot plate set to 70°C for 2 h to drive off the solvent. A similar deposition sequence yielded a 1.5 μm polymer layer on a test silicon wafer; thus we used this value in our calculations.

Results and discussion: Fig. 3 shows the result of a sensor test. The sensor was packaged in an airtight enclosure with fibre pigtails; a controlled mixture of air, water vapour and isopropanol was flowed through the package at the rate of 0.1 l/s. The water vapour concentration was held at 10 000 ppm (at 23°C) throughout the experiment. To facilitate readout we have tracked the position of one of the resonator peaks seen in Fig. 2 using a tunable laser. Isopropanol was introduced in 30 min pulses at various concentrations between 500 and 50 ppm, interspersed with 60 min intervals of clean air.

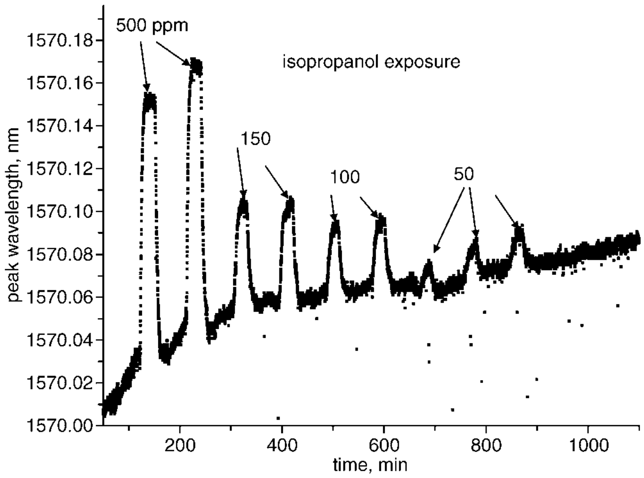

Fig. 3 *Results of chemical exposure experiment*
Water vapour concentration kept at 10 000 ppm

The chemical exposure resulted in easily detectable signals surpassing slow background variations. We attribute some of this background primarily to the sensor equilibration to the change in the water vapour concentration from room environment to the regulated 10 000 ppm level at the start of the experiment. The sensitivity is limited by short-term fluctuations in the measured peak position—we measured the noise of 8 pm rms during the gas flow. The noise dropped to 0.5 pm rms when we stopped the flow pointing to a problem with the fibre attachment and gas flow turbulence inside the sensor package. Solving this problem will improve the sensitivity sixteen fold.

Conclusions: The results demonstrate the promise of the ring-resonator-based chemical sensors. This technique may be applied to array sensing or to fabrication of single non-specific indicators. Since ethyl cellulose is known to respond to a wide variety of volatiles, the sensor reported here can be used as non-specific spill indicator for volatile compounds. The demonstrated sensitivity to isopropanol is 50 ppm, compared with the 400 ppm permissible exposure limit set by the US Occupational Safety and Health Administration, which makes this sensor immediately useful for health-related air monitoring.

Acknowledgment: This research was carried out at the Jet Propulsion Laboratory, California Institute of Technology, under a contract with the National Aeronautics and Space Administration.

5 November 2003
Electronics Letters online no: 20040062
doi: 10.1049/el:20040062

A. Ksendzov, M.L. Homer and A.M. Manfreda (*Jet Propulsion Laboratory, 4800 Oak Grove Drive, Pasadena, CA 91109, USA*)

E-mail: alexander.ksendzov@jpl.nasa.gov

References

1 Boyd, R.W., and Heebner, J.E.: 'Sensitive disk resonator photonic biosensor', *Applied Opt.*, 2001, **40**, (31), pp. 5742–5747
2 Krioukov, E., Klunder, D.J.W., Driessen, A., Greve, J., and Otto, C.: 'Sensor based on an integrated optical microcavity', *Opt. Lett.*, 2002, **27**, (7), pp. 512–514
3 Ryan, M.A., Homer, M.L., Buehler, M.G., Manatt, K.S., Lau, B., Karmon, D., and Jackson, S.: 'Monitoring space shuttle air for selected contaminants using an electronic nose'. Proc. 28th Int. Conf. on Environmental systems, Warrendale, PA, USA (Society for Automotive Engineers), 1998, Paper No. 981564
4 Gardner, J.W., and Bartlett, P.N.: 'Electronic noses: principles and applications' (Oxford University Press, New York, 1999)
5 Lonergan, M.C., Severin, E.J., Doleman, B.J., Beaber, S.A., Grubb, R.H., and Lewis, N.S.: 'Array-based vapor sensing using chemically sensitive, carbon black-polymer resistors', *Chem. Mater.*, 1996, **8**, pp. 2298–2312
6 Patel, S.V., Jenkins, M.W., Hughes, R.C., Yelton, W.G., and Ricco, A.J.: 'Differentiation of chemical components in a binary solvent vapor mixture using carbon/polymer composite-based chemiresistors', *Anal. Chem.*, 2000, **72**, pp. 1532–1542
7 Rafizadeh, D., Zang, J.P., Tiberio, R.C., and Ho, S.T.: 'Propagation loss measurements in semiconductor microcavity ring and disk resonators', *J. Lightwave Technol.*, 1998, **16**, (7), pp. 1308–1314